Evaluation of the Graphene Dispersions for Kevlar Fabrics Functionalization Obtained by the Liquid-Exfoliation of Graphite

Ieva Bake
Centre for Design and Technology
Institute of Arhitecture and Design
Riga Technical University
Riga, Latvia
ieva.bake@rtu.lv

Liga Rampane
Centre for Design and Technology
Institute of Arhitecture and Design
Riga Technical University
Riga, Latvia
liga.rampane@rtu.lv

Ilze Balgale
Centre for Design and Technology
Institute of Arhitecture and Design
Riga Technical University
Riga, Latvia
ilze.balgale@rtu.lv

Silvija Kukle
Centre for Design and Technology
Institute of Arhitecture and Design
Riga Technical University
Riga, Latvia
silvija.kukle@rtu.lv

Imants Adijans
Rezekne Academy of Technologies
Laser Technologies Research Center
Riga , Latvija
Imants.adijans@rta.lv

Abstract. The process where pristine graphite is subjected to a solvent treatment seems simple and scalable and has attracted the attention of researchers over many years. However, for successful exfoliation, overcoming the van der Waals attractions between the adjacent layers of graphite is necessary. Over time, several methods have been created to overcome the attraction between layers. Graphene's liquid phase exfoliation (LPE) occurs due to the strong interactions between the solvent molecules and the basal planes of graphite, overcoming the energetic resistance to exfoliation and subsequent dispersion. Ultra sonication used for exfoliation can produce single or few layered graphene flakes. During sonication the sound waves propagate through liquid medium in alternating high- and low-pressure cycles, strong mechanical and thermal energy released by acoustic cavitation results in splitting up large particles into fine ones and dispersing them. Simultaneous insertion of solvent and/or intercalation molecules in between the graphite layers takes place supporting graphite separation into graphene layers.
The dispersion capacity of graphene flakes depends on how appropriate the solvent properties are to the corresponding properties of graphene, such as surface tension, Hildebrand, and Hansen solubility parameters. Only certain solvents can disperse graphene well and form a dispersion appropriate for specific future applications. In addition, after exfoliation by ultra sonication graphene flakes aggregation due to the van der Waals attractions must be overcome to prepare in long-term stable dispersions of nanometres-size graphene sheets.
The research has focused on the preparation of stable dispersion ready for transfer without intermediate processes to the Kevlar fabrics. An experimental comparison of the potentials of the 4 solvents for the application resulted in three corresponding to the intended use, two of them examined in detail, supplementing the composition of the LPE liquid medium with triethanolamine to obtain sufficient performance graphene coverage on Kevlar textile fibres.
Keywords: Dispersion, Graphene, Solvents, Zeta potential.

I. INTRODUCTION

Enhanced mechanical properties of aromatic polyamide fibres or films can be very useful as ultra-strong membranes, coatings, and other advanced applications [1]. Carbon nanostructures is considered a promising ballistic protection material, due to their low density and excellent mechanical properties. Recent experimental and computational investigations on the behaviour of graphene (Gr) under impact conditions revealed exceptional energy absorption properties and suggest that superior performance can be obtained in ballistic applications by applying Gr nano-coatings over other materials. Recent experimental and computational investigations on the behaviour of graphene under impact conditions revealed exceptional energy absorption properties and suggests that superior performance can be obtained in ballistic applications by applying graphene nanocoating's on other materials [2]. A homogeneous and uniform dispersion of Gr on the matrix is required so that the external load may be efficiently transferred under the stress condition through strong interfacial interactions between Gr layers and the polymer. The inherent nature of

Print ISSN 1691-5402
Online ISSN 2256-070X
https://doi.org/10.17770/etr2024vol1.7985

Gr, however, makes its dispersion difficult within the majority of polymers [3]. The non-covalent bonding of pristine Gr can be developed with aromatic polyamides that have extended aromatic rings on the chain of molecules, as they have highly mobile electrons π and π* located on their chains. The multiple π–π interactions between the exfoliated layer's crystalline structure of Gr and aramids can provide improvement in the mechanical properties [4]. To ensure this an appropriate dispersant–solvent system that interacts with the graphene and Kevlar fibre's surface must be selected to improve the liquid medium interface properties and realize the uniform and stable dispersion of graphene [5].

Due to the existing industrial knowledge and equipment, graphite liquid exfoliation is possibly the most viable option for upscaling graphene production. Graphene's liquid phase exfoliation (LPE) occurs due to the strong interactions between the solvent molecules and the graphitic basal planes, overcoming the energetic resistance to exfoliation and subsequent dispersion [6].

The principle of LPE lies in assisting the separation between graphene layers held together by electrostatic attractions that require strong mechanical force to separate [7]. To reduce this energy, the attractive forces holding layers of graphene together must be disrupted. This is done by first dispersing graphite flakes into liquid media, followed by graphite intercalation (division into microlayers) and microlayers exfoliation. At the final stage, maintaining a stable dispersion of isolated flakes in a liquid medium must be ensured (Fig.1). The challenge is that graphene suffers from a limited dispersibility even in its suitable solvents, which is due to the small mixing potential and strong π-π attraction between two-dimensional graphite structures. Several studies have shown graphite can be exfoliated in liquid environments by using ultrasound to extract individual layers [8]. In this case LPE involves three steps: the dispersion of graphite in a solvent; the exfoliation of dispersion via sonication; the dispersion stabilization (Fig.1).

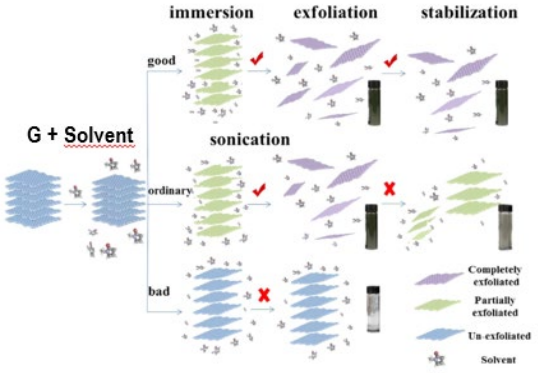

Fig.1. LPE involves three main steps: The dispersion of graphite in a solvent; The exfoliation of dispersion via sonication; the dispersion stabilization [9]

During sonication, ultrasonic waves produce in the liquid medium local compressions and rarefactions, forming vacuum cavities which then collapse, generating high pressure jets. These jets peel off graphene layers from graphite and weaken the Van der Waals interaction between the layers. The intercalation of solvent molecules between graphitic planes allows for further exfoliation and consequent stabilization of dispersion [10]. Attention must be paid to the choice of the dispersing solvent as the solvent is a crucial factor in the exfoliation process, and to be effective, it must comply with three main requirements: transmit the exfoliating power efficiently, minimize the energy needed to disrupt the van der Waals forces among layers and stabilize the exfoliated layers by providing steric hindrance to prevent re-agglomeration [11].

Matching an appropriate graphene dispersant–solvent system, the potential energy studies of the graphene surface and its relationship with the potential energy of the dispersant–solvent system were carried, eventually believing that the stability of the graphene dispersion and dispersant–solvent system is characterized by Hansen's solubility coefficient [12] and a three-dimensional representation of Hildebrand solubility parameters - the dispersion (δd), polar (δp) and hydrogen bonding (δh) interactions in the Hansen 3D space is considered as framework to predict if and how a material will disperse in a particular solvent and form a solution [13, 14]. Typically, 1-methyl-2-pyrrolidone (NMP) or dimethylformamide (DMF) is used as a solvent in LPE since both are successful for exfoliating graphite and producing stable dispersions of graphene. et al., boiling point of these solvents make them difficult to remove and results in major material loss and degradation of quality, the generation of toxic waste [15, 16] turning to the feasibility research of replacing NMP and DMF with green solvents. A group of scientists [14] has released Dihydrolevoglucozenone (Cyrene) as one of the most performant graphene solvents in a large-scale comparative analysis of possible solvents.

Biological solvent Cyrene is extracted from cellulose in a two-step process using the levoglucosenone (biomass) process, which at the same time guarantees a low environmental impact and economic feasibility. Cyrene is a waste-derived and fully biodegradable seven-membered heterocyclic cycloalkanone which is fully biodegradable an environmentally friendly [17] alternative to dimethylformamide (DMF) and N-methyl-2- pyrrolidine (NMP). It is miscible with water and many organic solvents. Unlike traditionally used polar aprotic solvents, the Cyrene molecule does not contain nitrogen and sulphur heteroatoms [18]. As part of a previous study, the possibility of creating a Cyrene-based dispersion and para-aramid fabric variants modified with it has been demonstrated [19].

Given the hitherto approved use of solvent DMAc in aramid and other textile fibres obtaining processes, it would be premature to exclude it from comparative studies, especially since its solubility parameters are also relatively close to those of graphene (Table 1).

N, N-Dimethylacetamide DMAC is a dipolar aprotic solvent used in many organic reactions and for industrial purposes. It is a universal solvent due to its high boiling point, good thermal and chemical stability. It is indispensable in the processes of obtaining many textile fibres, used as a solvent for producing fibres and for organic compounds synthesis. Its broad range of miscibility makes it useful in mixed solvents. It is also stable to strong bases but hydrolyses in the presence of acids.

TABLE 1. HILDEBRAND SOLUBILITY PARAMETERS, SURFACE TENSION AND VISCOSITY OF USED SOLVENTS

	Solubility parameters, $MPa^{0.5}$				**Surface tension, mN.m-1**	**Viscosity, g·s-1·m-1**
	δ_D	δ_P	δ_H	R		
Graphene	18	9.3	7.7	-	46.7	-
DMAc	16.8	11.5	9.4	3.7	32.4	0.9
Cyrene [11]	18.8	10.6	6.9	2.2	33.6	14.5
TEA	17.3	7.6	21	-	45.9	607*

*TEA viscosity dramatically decreases with temperature increase.

Although previous studies had shown that green solvents can be used to produce graphene by means of LPE, it has not progressed much further. To enhance the graphene yield in green solvent LPE, which currently is ca. 50−75% lower than in DMF or NMP [20., 21], additives such as surfactants and/or dispersants have been intensively explored [22]. Key factors that influence the graphene yield in LPE - *exfoliation efficiency*, and the *dispersibility* of the solvent could be considered [23].

Given DMAc's low dynamic viscosity (Table 1) and based on previous successful experience of incorporating triethanolamine (TEA) into dispersion and improved adhesion to the modifiable Kevlar fabric fibres surface [19], both variants of the comparable solvent-based liquid medium included TEA (Table 1).

TEA is a viscous organic compound that is both a tertiary amine and a triol - a molecule with three groups of alcohol. As amine, TEA can accept hydrogen and as a surfactant, it can reduce the interphase stress in the mixture or solution, preventing the emulsion from layering or the deposition of compounds from the solution. TEA offers close correspondence of δD and δP to Gr and Cyrene, and as a nucleophile exhibits a much higher δH (Table 1), suggesting the ability to bind to the desired molecule more easily in the coating process. There are no examples of successful TEA use in previous studies related to the Gr extraction.

II. MATERIALS AND METHODS

1) Theoretical Methods

Viscosity Determination of Liquid media

To determine the particle sizes and their distribution in dispersion, viscosity values of the solutions to be measured are required. Since the liquid medium of the dispersion (suspension) to be analysed often consists of mixtures of solvents, viscosity values could not be obtained from the literature, they had to be determined experimentally. In a rotational type of viscometer, speed is controlled, corresponding to its force measurement is used to calculate viscosity, which is necessary to ensure the rotation of a solid body in a viscous environment. This viscometer type proved to be inadequate for the dispersions to be tested, as large volumes are required to obtain stable measurements and very low viscosities difficult to measure with sufficient accuracy. Instead, the method of falling ball was used.

The solution to be analysed is poured into a capillary, a ball of stainless steel is placed in it. The falling ball micro viscometer measures the time t required for the ball to move from one end to the other in the capillary (Fig. 2.). This measurement principle also ensures that the measurement requires a small sample volume – already around 1 mL is sufficient to obtain the measurement. The dynamic viscosity by this method is calculated according to equation (1):

$$\eta = \left(\frac{1}{6\pi v}\right)[4/3\pi r 2(\sigma - \rho)g], \quad (1)$$

where - η, Pa s; r - the sphere's radius (m), σ - the density of the sphere (kg/m^3), ρ - the density of the liquid (g/ml), g: acceleration due to gravity (9.81 m/s^2), v - the terminal velocity of the sphere (m/s).

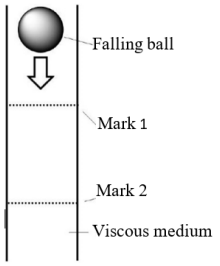

Fig.2. Viscosity method testing scheme.

Characterization of Nanoparticles and Microparticles

The LitesizerTM 500 is designed to characterize particles in liquid dispersions. Instrument makes it possible to determine particle sizes, ζ-potential and molecular weight by measuring dynamic (DLS), electrophoretic (ELS) and static light scattering (SLS), as well as sample light transmission and refractive index. The equipment operates on the principle of scattering dynamic light: the smaller the particles, the higher the speed of Brown's movement in the liquid. By measuring the change in light scattering, which depends on the speed of movement of particles, it is possible to calculate particle sizes and characterize the particle size distribution. The distribution of dispersed particles is characterized by particle diameters, while the scattering of diameters with the Polydispersity Index.

The hydrodynamic diameter of the particles is measured together with the layers surrounding the particles in solution (Fig. 3). The Polydispersity Index PDI is calculated, equation (2):

$$PDI = (\frac{\sigma}{d})^2, \quad (2)$$

where σ is particle size standard deviations (nm), d average particle diameter (nm).

The PDI value can vary from 0 to 1: if the PDI of colloidal particles is less than 0.1 (10%) the dispersion contains monodispersed particles, and if the PDI value exceeds 0.1, this may mean the size distribution of polydisperse particles. International Organizations for

Standardization have determined that PDI values of < 0.05 (5%) are more common for monodispersible samples, while values of > 0.7 (70%) are common for a broad particle size distribution, so the corresponding variances are classified as highly polydisperse [24] standard. It should be noted that polydispersity may occur due to particle size distribution in the sample, as well because of agglomeration or aggregation of the sample during isolation or analysis of the sample.

The physical properties of suspensions (nanoparticles) and colloids largely depend on the interface properties of particles and liquids, knowing the potential of Zeta is important for their assessment. From the fundamental theory's perspective, zeta (ζ) potential is the electrical potential in the interfacial double layer at the location of the slipping plane (Figure 3). Thus, zeta potential can be regarded as the potential difference between the dispersion medium and the stationary layer of the fluid attached to the particle layer.

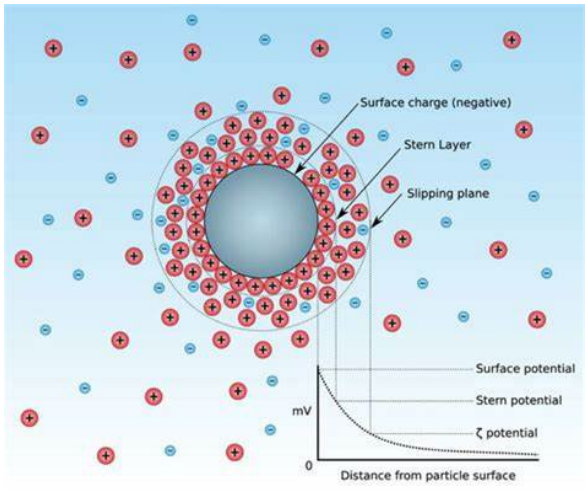

Fig.3. Potentials difference of a particle suspended in a dispersion media as a function of distance from the charged particle surface [25]

ζ-potential describes the electrochemical balance at the particle-liquid interface by measuring the magnitude of electrostatic repulsion/attraction between particles. Thus, it has become one of the basic parameters for assessing the stability of colloidal particles. ζ- potential cannot be directly measured. It is calculated according to theoretical models or calculated from experiments, often based on the mobility of electrophoresis.

In capillary electrophoresis the sample is injected into a buffered solution filled in a capillary tube. When an electric field is applied to the capillary tube, the sample's components migrate in result of electrophoretic mobility and electroosmotic flow.

Electrophoretic mobility is the solute's response to the applied electrical field in which cations move toward the negatively charged cathode, anions move toward the positively charged anode, and neutral species remain stationary. The other contribution to a solute's migration is electroosmotic flow, which occurs when the buffer moves through the capillary in response to the applied electrical field. Under normal conditions the buffer moves toward the cathode, sweeping most solutes, including the anions and neutral species, toward the negatively charged cathode. Basically, to determine the zeta potential, the speed with which a charged particle moves in response to an electric field electrophoretic velocity is measured, equation (3):

$$\upsilon ep = \mu ep\, E \qquad (3)$$

where μep is the solute's electrophoretic mobility ($mm^2h^{-1}v^{-1}$), and E is the magnitude of the applied electrical field (N/C). A solute's electrophoretic mobility is defined as:

$$\mu ep = q/6\pi\eta r \qquad (4)$$

where q is the solute's charge (C), η is the buffer's viscosity (Pa s), and r is the solute's radius (mm).

The migration rate is proportional to ζ-potential. Speed is usually measured using a laser doppler anemometer. The calculation is based on the theory described by Marian Smoluchowski in 1903 [26]. Smoluchowski's theory is valid for any concentration or shape of dispersion particles. However, it takes on a sufficiently thin double layer and ignores any surface conductivity.

ζ-potential, also known as electrokinetic potential, is measured in millivolts (mV). When the zeta potential is equal to zero, the colloid precipitates to a solid state.

0 to ± 5 mV, rapid coagulation or flocculation occurs (the formation of flaky aggregates in solution);

±10 to ± 30 mV initial area of stability;

±30 to ± 40 mV moderate stability;

±40 to ± 60 mV good stability;

Above ± 61 mV excellent stability [25].

2) Experimental Methods

The Table 2 shows dispersion comparison, and they process parameters, where US (ultra sonification) and C (centrifuge) was applied.

TABLE 2 DISPERSIONS COMPOSITION AND PROCESSING PARAMETERS [27]

	Variants designation			
	G-DMAc-TEA_d1	**G-DMAcb-TEA2_d2**	**G-CIR-TEA_d3**	**G-CIRb-TEA2_d3**
Graphite, Wt., %	2*	25**	2*	25**
DMAc, Wt., %	78	60	-	-
Cyrene, Wt., %	-	-	80	50
TEA, Wt., %	20	15	18	25
US, min	60	30	60	30
C, min/ rad $^{s-1}$	20/272	20/126	20/272	20/126

* Pristine graphite flakes
** Recovered sediments

Graphite flakes, 99% carbon basis, -325 mesh particle size (≥99%), natural (Sigma-Aldrich)

The densities of the dispersions d1 and d2 are 0.968 and 0.973 g/mL, respectively (DMAc 0.937 g/mL). The densities of the Cyrene-based dispersions d3 and d4 are 1.258 and 1.257 g/mL, respectively (Cyrene 1.25 g/mL).

Viscosity measurements carried out with a viscometer Lovis 2000 M/ME (Anton Paar) at 20 °C.

Particle size analysis and ζ- potential has been determined with the LitesizerTM 500 instrument (Anton Paar) using appropriate software.

Particle size measurements performed on undiluted samples. ζ- Potential measurements made with samples at a 1: 30 dilutions. Samples for the tests were taken with a disposable pipette from the upper part of the tube before settling the samples for at least one hour. Glass cuvettes were used for measurements. The dispersion cells were in a thermostatic chamber at 20 °C during the test process. A series of measurements have been carried out for each sample, from which the distribution of the average dimensions and ζ- potential have been calculated.

III. DISCUSSION

High viscosity is, in principle, beneficial for the LPE process, as it increases the outcome of exfoliation and reduces the proportion of defects and sediments. However, too high viscosity contributes to the stable retention of coarse particles and agglomerates in dispersion by centrifugation of them, thus not separating them from the desired thinner and lightest flakes. The measurements of the dynamic viscosity of the four dispersions considered are very different. The viscosity of DMAc-based dispersions 1.89 mPa-s and 2.17 mPa-s after re-dispersion of recovered sediments confirms the above about the possible effect of components viscosity on the dispersion parameters (Table 2). By adding the modifier TEA to the liquid medium, it has succeeded in increasing the low viscosity of DMAc (Table 1) to the level required in subsequent modification processes of Kevlar fabric (Table 3).

TABLE 3 PARAMETERS CHARACTERIZING THE DISPERSIONS TO BE COMPARED

	G-DMAc-TEA_d1	G-DMAcb-TEA2_d2	G-CIR-TEA_d3	G-CIRb-TEA2_d4
Viscosity, mPa-s	1.89	2.17	99.4	231
HYDRO Ø, nm	387	392	1668	392
Polydispersity index, %	27.7	25.3	164.7	25.3
Diffusion coefficient, µm²/s	0.6	0.5	0	0
Deciles, nm				
D1	195	179	954	231
D5*	333	309	1359	332
D9	511	645	2159	514
Interdecile range, nm I_{80}	315	466	1205	283
Modal, nm	358	379	1528	369

*) D5 = median

Polidispersity indexes of dispersions d1 and d2 between 25% and 28% are well below the 70% limit of common for a broad particle size distribution. Figure 4 graph (a) and median < modal < mean particle sizes values (Table 3) suggest right side asymmetry of dispersion d1 particle sizes distribution, 80% of particle sizes located in a range between 195 and 511 nm. In turn, recovered sediment dispersion's d2 80% of particle sizes located in a wider interval between 179 and 645 nm, I_{80} increased by 1.5 times while the right-side particle sizes distribution asymmetry remains (Figure 4, b).

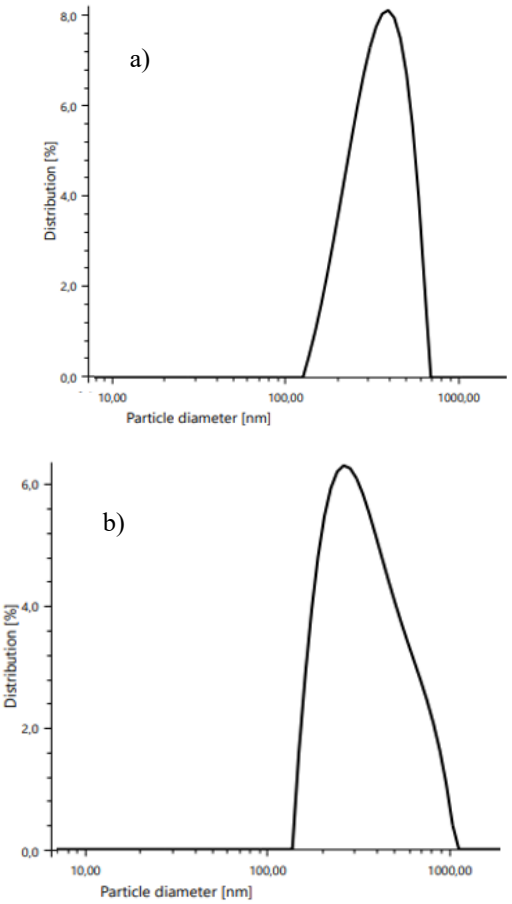

Fig.4. DMAc based dispersions particle size distribution by intensity, a) G-DMAc-TEA_d1, b) G-DMAcb-TEA2-d2.

Considering that the viscosity of Cyrene is almost 15 times higher than that of DMAc, while the viscosity of TEA is highly dependent on the temperature at the time of measurement (20 °C), it is necessary to look very carefully at the obtained measurements of the dynamic viscosity of both Cyrene based dispersions respectively 99.4 and 231 mPa-s (Table 3), especially in cases where the further processing takes place at temperatures above 50 °C.

Obtained PDI 165% of Cyrene based dispersion d3 indicates a broad graphene particle size distribution (Table 3). The graph of the image shows d3 distribution strongly shifted to a larger particle sizes area (Figure 5, top), with 80 % of the particle diameters in the range 954 to 2159 nanometres (Table 3) testifying to the exfoliated graphene layers agglomeration and aggregation during d3 samples isolation, transportation, and analysis. The measurements obtained suggest that graphite layers are partially exfoliated and perhaps the viscosity and other parameters of liquid media has not been sufficient to ensure dispersion d 3 stability. The assumption is confirmed by the relatively high viscosity of the dispersion d4, its corresponding PDI value of 25% and the other parameters characterizing the distribution, which differ only slightly

from the corresponding indicators of dispersions d1 and d2. The interdecial range I_{80} of 283 nm that measures particle size variance is even lower compared to d1 and d2 I_{80} scores of 315 and 466 nm respectively.

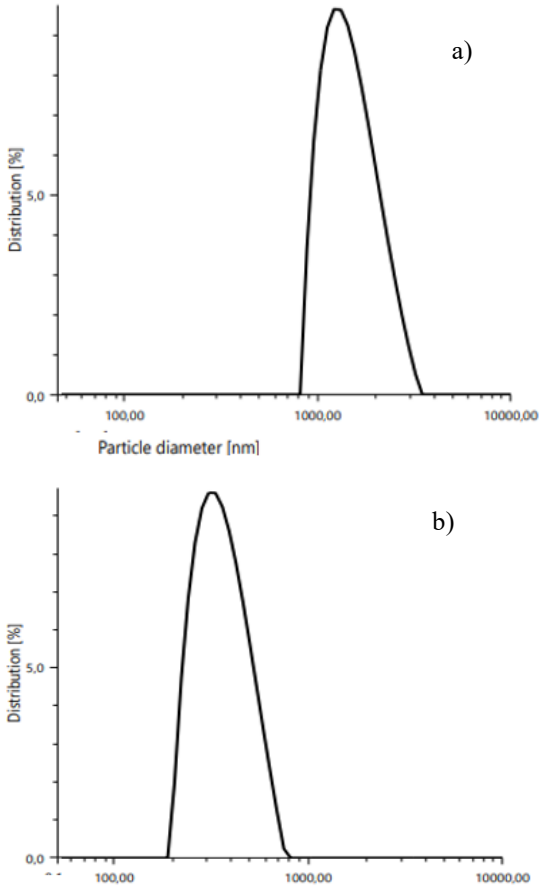

Fig. 5. Cyrene based dispersions particle size distribution by intensity, a) G-CIR-TEA_d3, b) G-CIR-TEA2-d4.

This could be explained by a significant increase in d4 viscosity due to changes in the proportions of the liquid medium composition: reduced the concentration of Cyrene from 80 wt% to 50 wt%, while the concentration of TEA increased from 18 to 25wt%.

The ζ-potential of the dispersion d1 at the peak of the distribution curve (Figure 6, a) and the mean values (-35.5) and (-39.4) mV, respectively, indicate the stability of DMAc-based dispersion d1 which has also been confirmed in by ensuring d1 shelf life at least one month. From the sediments obtained by centrifugation re-dispersion d2 values of the ζ-potential distribution peak (Figure 6, b) and the average zeta potential values respectively -44.6 and -43 mV are relatively higher, which is explained by repeated exposure to sonication. Experience gained during the experiments has shown that sediments re-dispersion allows fabric coatings richer in graphene [27].

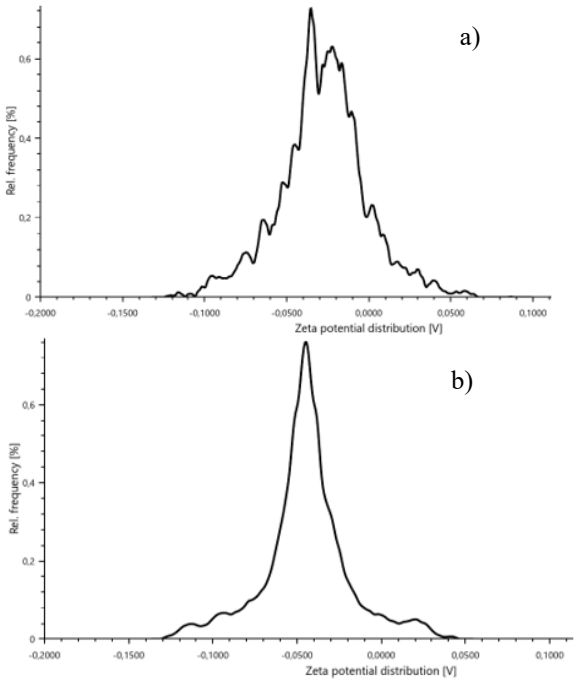

Fig. 6. DMAc solvent based dispersions ζ-potential distributions, a) G-DMac-TEA-d1, b) G-DMAcb_TEA2_d2.

The ζ-potential distributions of both solvent Cyrene based dispersions d3 and d4 failed to obtain by confirming the rapid dispersion stratification observed in practice and the formation of agglomerates. This is explained by the definition that the efficacy of exfoliation is determined by the solvent's capacity to separate individual layers of graphene from graphite flakes, but the graphene dispersibility is the solvent's ability to form uniform and stable graphene dispersions over a given time. The limited dispersibility of the graphene in green solvents is hindered by the limited dispersibility of the obtained graphene flakes in them. This means that these dispersions should be used immediately after preparation, but as practice shows the expected result cannot always be obtained.

IV. CONCLUSIONS

In order to predict the compliance of the dispersing solvent system with graphene exfoliation, the researchers have studied the potential energy of the graphene surface and its relationship to the potential energy of the dispersing system for a long time, ultimately believing that three-dimensional representation of Hildebrand solubility parameters interactions in the Hansen 3D space offered a framework to predict if and how a material will disperse in a particular solvent and form a solution.

Despite numerous studies the liquid-phase dispersion of graphene is still the core problem that must be overcome in the experimental studies of nanomaterials and matching the properties of the resulting dispersion with the application in subsequent technological processes to promote its industrial uses.

Creating a technological sequence in which pristine graphite is directly subjected to a solvent treatment and production of exfoliated graphene sheets in the form of stable dispersion suitable for an immediate modification of Kevlar fabric a very important aspect is the dispersion ability to provide Gr particles bonding to the fibres of the

modifiable material at the nano/micro level. It is supposed the non-covalent bonding development in result of multiple π–π interactions between the exfoliated Gr particles and highly mobile pi electrons on aromatic rings of Kevlar molecule chains which ensures strong adhesion of the coating by modifying Kevlar fabric with the DMAc-based dispersion.

A comparative analysis of the two types of dispersions presented in the article based on experimental studies shows that the solvent Cyrene- based liquid media can provide Gr exfoliation from graphite flakes, especially after sediments re-dispersion obtaining an equivalent with the DMAc based liquid media Gr particle size distribution and equal PI 25.3% for dispersions d2 and d4. Mean value of Zeta potential of DMAc-based dispersions of d1 is (-39) mV (moderate stability) and increase after sediments re-dispersion till (-43) mV (good stability).

At the same time Gr dispersibility is low because Cyrene, as a solvent, does not provide the electrochemical balance at the particle-liquid interface necessary for stable Gr particles dispersion, resulting in the rapid agglomeration of exfoliated particles and dispersion stratifying. Exploring potential of Zeta of the proposed dispersions in parallel with the studies of the potential energy of the graphene surface and its relationship with the potential energy of the dispersant–solvent system can greatly facilitate the efforts into finding suitable and sustainable solvent alternatives.

In addition, the dispersion dynamic light scattering analysis system allows to evaluate the size distribution of particles suspended in a dispersion media and analyses the parameters characterizing the distribution, which allows optimizing the dispersing solvent system according to the intended use.

ACKNOWLEDGEMENTS

The authors thank the funder for awarding the grant within the framework of project No. VPP-AIPP-2021/1-0009 of the Latvian National Research Programme: Defence Innovation Research Programme.

The authors also express their gratitude to the Institute of Solid State Physics, University of Latvia for the opportunity to measure the dispersion parameters.

REFERENCES

[1] Yang, M.; Cao, K.; Sui, L.; Qi, Y.; Zhu, J.; Waas, A.; Arruda, E.M.; Kieffer, J.; Thouless, M.; Kotov, N.A. *Dispersions of aramid nanofibers: A new nanoscale building block*. ACS Nano 2011, 5, 6945–6954.

[2] Rafael A. Bizao, Leonardo D. Machado, Jose M. de Sousa, Nicola M. Pugno & Douglas S. Galvao. *Scale Effects on the Ballistic Penetration of Graphene Sheets*. 2018, Scientific Reports (nature.com).

[3] Stankovich, S.; Dikin, D.A.; Dommett, G.H.; Kohlhaas, K.M.; Zimney, E.J.; Stach, E.A.; Piner, R.D.; Nguyen, S.T.; Ruoff, R.S. *Graphene-based composite materials*. Nature 2006, 442, 282. 33.

[4] Georgakilas, V.; Otyepka, M.; Bourlinos, A.B.; Chandra, V.; Kim, N.; Kemp, K.C.; Hobza, P.; Zboril, R.; Kim, K.S. *Functionalization of graphene: Covalent and non-covalent approaches, derivatives, and applications*. Chem. Rev. 2012, 112, 6156–6214.

[5] Ma, L.; Zhao, D.; Zheng, J. *Construction of electrostatic and π–π interaction to enhance interfacial adhesion between carbon nanoparticles and polymer matrix*. J. Appl. Polym. Sci. 2019, 137, 48633.

[6] Kadir Bilisik and Mahmuda Akter. *Graphene nanocomposites: A review on processes, properties, and applications.* 2022, Journal of Industrial Textiles 51(3S) Vol. 51(3S) 3718S–3766S. DOI: 10.1177/15280837211024252.

[7] D. G. Papageorgiou, I. A. Kinloch, and R. J. Young, *"Mechanical properties of graphene and graphene-based nanocomposites,"* Prog. Mater. Sci., vol. 90, pp. 75–127, 2017, doi: 10.1016/j.pmatsci.2017.07.004.

[8] C. Vacacela Gomez et al., *"The liquid exfoliation of graphene in polar solvents,"* Appl. Surf. Sci., vol. 546, p. 149046, 2021, doi: https://doi.org/10.1016/j.apsusc.2021.149046.

[9] M. Eredia, A. Ciesielski, and P. Samorì, *"Graphene via Molecule-Assisted Ultrasound-Induced Liquid-Phase Exfoliation: A Supramolecular Approach,"* .Phys. Sci. Rev., vol. 1, no. 12, pp. 55–57, 2016, doi: 10.1515/psr-2016-0101.

[10] J. Shen et al., *"Liquid Phase Exfoliation of Two-Dimensional Materials by Directly Probing and Matching Surface Tension Components"*. Nano Lett., vol. 15, no. 8, pp. 5449–5454, Aug. 2015, doi: 10.1021/acs.nanolett.5b01842.

[11] L. I. Silva, D. A. Mirabella, J. Pablo Tomba, and C. C. Riccardi, *"Optimizing graphene production in ultrasonic devices"*. Ultrasonics, vol. 100, p. 105989, Jan. 2020, doi: 10.1016/j.ultras.2019.105989.

[12] R. Banavath, S. S. Nemala, R. Srivastava, and P. Bhargava, *"Non-Enzymatic H2O2 Sensor Using Liquid Phase High-Pressure Exfoliated Graphene"* .J. Electrochem. Soc., vol. 168, no. 8, p. 86508, Aug. 2021, doi: 10.1149/1945-7111/ac1eb6.

[13] Lim, H. J., Lee, K., Cho, Y. S., Kim, Y. S., Kim, T., and Park, C. R. (2014). *Experimental consideration of the Hansen solubility parameters of as-produced multi-walled carbon nanotubes by inverse gas chromatography.* Phys. Chem. Chem. Phys. PCCP. 16, 17466–17472. doi: 10.1039/C4CP02319F).

[14] C. M. Hansen, *Hansen solubility parameters: A user's handbook: Second edition*. 2007. doi: 10.1201/9781420006834.

[15] H. J. Salavagione et al., *"Identification of high performance solvents for the sustainable processing of graphene"*. Green Chem., vol. 19, no. 11, pp. 2550–2560, 2017, doi: 10.1039/c7gc00112f.

[16] Tyurnina, Anastasia & Tzanakis, Iakovos & Morton, Justin & Mi, Jiawei & Porfyrakis, Kyriakos & Maciejewska, Barbara & Grobert, Nicole & Eskin, Dmitry. (2020). *Ultrasonic exfoliation of graphene in water: A key parameter study*. Carbon. 168. 10.1016/j.carbon.2020.06.029.

[17] Anastasia V. Tyurnina, Justin A. Morton, Tungky Subroto, Mohammad Khavari, Barbara Maciejewska, Jiawei Mi, Nicole Grobert, Kyriakos Porfyrakis, Iakovos Tzanakis, Dmitry G. Eskin, *Environment friendly dual-frequency ultrasonic exfoliation of few-layer graphene*, Carbon, Volume 185, 2021, Pages 536-545, ISSN 0008-6223.

[18] J. Sherwood et al.,*"Dihydrolevoglucosenone (Cyrene) as a bio-based alternative for dipolar aprotic solvents"*. Chem. Commun. (Camb)., vol. 50, no. 68, pp. 9650–9652, Sep. 2014, doi: 10.1039/c4cc04133j.

[19] A. D. Curzons, D. C. Constable, and V. L. Cunningham, *"Solvent selection guide: a guide to the integration of environmental, health and safety criteria into the selection of solvents"*. Clean Technol. Environ. Policy, vol. 1, no. 2, pp. 82–90, 1999, doi: 10.1007/s100980050014.

[20] S. Kukle, I. Bake, and L. Abele*, "Graphene-containing para aramid fabric coating via surfactant assisted exfoliation of graphite"*. Mater. Today Proc., vol. 97, pp. 44–51, 2024, doi:https://doi.org/10.1016/j.matpr.2023.09.131.

[21] O'Neill A. *'Liquid phase exfoliation of two dimensional crystals'*, [thesis], Trinity College (Dublin, Ireland). School of Physics, 2013, pp 158.

[22] Yi, M.; Shen, Z.; Zhang, X.; Ma, S. *Achieving Concentrated Graphene Dispersions in Water/Acetone Mixtures by the Strategy of Tailoring Hansen Solubility Parameters*. J. Phys.D: Appl. Phys. 2013, 46, 025301.

[23] Kai Ling Ng, Barbara M Maciejewska, Ling Qin, Colin Johnston, Jesus Barrio, Maria-Magdalena Titirici, Iakovos Tzanakis, Dmitry G Eskin, Kyriakos Porfyrakis, Jiawei Mi, and Nicole Grobert. *Direct Evidence of the Exfoliation Efficiency and Graphene Dispersibility of Green Solvents toward Sustainable Graphene Production*. ACS Sustainable Chem. Eng. 2023, 11, 58−66.

[24] "ISO 22412:2017 - *Particle size analysis — Dynamic light scattering (DLS)*".

[25] A.Raja, Pavan; Barron, *"Physical Methods in Chemistry and Nano Science"*. OpenStax CNX, 2019, [Online]. Available: https://espanol.libretexts.org/Quimica/Química_Analítica/Métodos_Físicos_en_Química_y_Nano_Ciencia_(Barron)/01%3A_Análisis_Elemental/1.04%3A_Introducción_a_la_Espectroscopia_de_Absorción_Atómica.

[26] A. Fulinski, *"On Marian Smoluchowski's life and contribution to physics"* .Acta Phys. Pol. B, vol. 29, no. 6, pp. 1523–1537, 1998.

[27] L. Ābele, I. Baķe, L. Vilcēna, and S. Kukle, *"Development of Graphene-Based Functional Coating for the Surface Modification of Textiles".* Mater. Sci. Forum, vol. 1104, pp. 77–85, Nov. 2023, doi: 10.4028/p-i7kXSV.